

A contribution to the understanding of late Pleistocene dune sand-paleosol-sequences in Fuerteventura (Canary Islands)



Dominik Faust^{a,*}, Yurena Yanes^b, Tobias Willkommen^a, Christopher Roettig^a, Daniel Richter^{d,e}, David Richter^a, Hans v. Suchodoletz^c, Ludwig Zöller^d

^a Lehrstuhl Physische Geographie, TU Dresden, Germany

^b Department of Geology, University of Cincinnati, Cincinnati, OH 45221, USA

^c Professur für Physische Geographie, Universität Leipzig, Germany

^d Lehrstuhl Geomorphologie, Universität Bayreuth, Germany

^e Max-Planck Institute for Evolutionary Anthropology, Leipzig, Germany

ARTICLE INFO

Article history:

Received 27 July 2014

Received in revised form 9 June 2015

Accepted 14 June 2015

Available online 18 June 2015

Keywords:

Eolian deposits

Morphodynamics

Chronostratigraphy

Paleoclimate

Fuerteventura

ABSTRACT

This paper describes dune sand-paleosol-sequences of four pits in Northern Fuerteventura (Canary Islands). The elaborated stratigraphy is reinforced with luminescence dating to provide a first chronological estimation. Apart from a Holocene colluvial layer, the sequence spans the period from ca. 50 ka to ca. 280 ka. Paleosols were formed during glacial times and point to a standstill in sand supply. The isotopic composition of terrestrial gastropod shells retrieved from soil horizons reflects fluctuations in humidity conditions during different edaphic phases. Because eolian sands were deposited during glacial times as well, it is inferred that soil development was simply caused by a decrease in sand supply independent of climate change. Our geomorphic, geochronological and isotopic results are discussed considering different perspectives of dune sand-paleosol intercalation and more broadly, soil-forming conditions in general.

© 2015 Elsevier B.V. All rights reserved.

1. Introduction

Dune sand-paleosol-sequences in lower latitudes are considered to reflect changes in the environmental conditions (Petit-Maire et al., 1986; Tripaldi and Forman, 2007; Fitzsimmons et al., 2009; Roskin et al., 2011). Traditionally, the interpretation of such changes is understood through the concept of geomorphic activity linked to dune sand accumulation vs. geomorphic stability characterized by soil formation (Rohdenburg, 1970), which suggests climate driven changes in geodynamics. However, more recently has been suggested that the change from sand deposition to soil formation in some cases is first of all a question of sand availability (Roskin et al., 2013). Moreover, not all brownish or reddish layers intercalated between dune sands are soils that were formed in situ, instead they can be soil sediments (Roskin et al., 2013; Faust et al., 2014). Thus, the interpretation of sand-paleosol sequences in terms of paleoenvironmental changes appears to be more complicated than formerly assumed. On the Canary Islands, the occurrence of kaolinite and the increase of Al-content in dune sand, interbedded soils and soil sediments can be attributed to

the input of Saharan dust (locally called *calima*; Suchodoletz et al., 2009; Criado et al., 2011).

Previous stratigraphic and geochronological studies from the eastern Canary Islands mostly encompassed the period from the late MIS 3 until the Holocene (e.g. Meco and Pomel, 1985; Petit-Maire et al., 1986; Rognon et al., 1989; Damnati et al., 1996; Meco et al., 1997; Coello et al., 1999; Ortiz et al., 2006). This is due to the fact that most of these studies used radiocarbon dating of terrestrial gastropod shells to establish the chronology, an analytical method that only dates material younger than ~50,000 years and that furthermore appears to produce biased results in arid and semi-arid environments (Singhvi and Krubetschek, 1996). Hence, the reliability of already published ages has been debated over the last 10 years (e.g. Bouab and Lamothe, 1997; Meco et al., 2002, 2008; Suchodoletz et al., 2012; Faust et al., 2014). Meco et al. (2008), Damnati et al. (1996), Bouab and Lamothe (1997) and Ortiz et al. (2006) worked in two of the sand pits also investigated in this study (Melian and Costilla; see their Fig. 2) in northern Fuerteventura but used different dating methods (amino acid racemization, ¹⁴C, U–Th, OSL and IRSL), whereas Bouab (2001) and Meco et al. (2008) present OSL ages from the Costilla profile (see their Fig. 8) that are comparable with the data presented in this study. Other previous studies (Bouab and Lamothe, 1997; Ortiz et al., 2006) proposed age models that differ notably from our own age results. Furthermore,

* Corresponding author.

E-mail address: dominik.faust@tu-dresden.de (D. Faust).



Fig. 1. Location of the studied sand pits.

recent chronological data by Gutiérrez-Elorza et al. (2013) from the same quarries show “OSL” ages that must be regarded as questionable due to the lack of any methodic or stratigraphic documentation (see also comments by Faust et al., 2014).

Suchodoletz et al. (2008, 2012, 2013) presented OSL, IRSL and ESR ages of hillwash sediments (locally called Vega sediments) that were dammed up by volcanoes, and of dune sediments from the Mala Dune complex (Suchodoletz et al., 2013) that are all located on Lanzarote Island. These studies stressed the difficulties in establishing a robust chronology of Quaternary eolian deposits and paleosols from the

eastern Canary Islands due to the rarity of suitable material for luminescence dating.

In this study we present new comprehensive geomorphological, stratigraphic and paleoenvironmental data reinforced with new IRSL dates covering the last ca. 250 ka from four large sand pits in northern Fuerteventura (Fig. 1), two of which have never been studied by previously published work. Based on new multi-proxy data this investigation aims to build up a composite stratigraphy and should help to clarify the chronological frame of four important Quaternary eolian deposits from Fuerteventura. A robust and improved

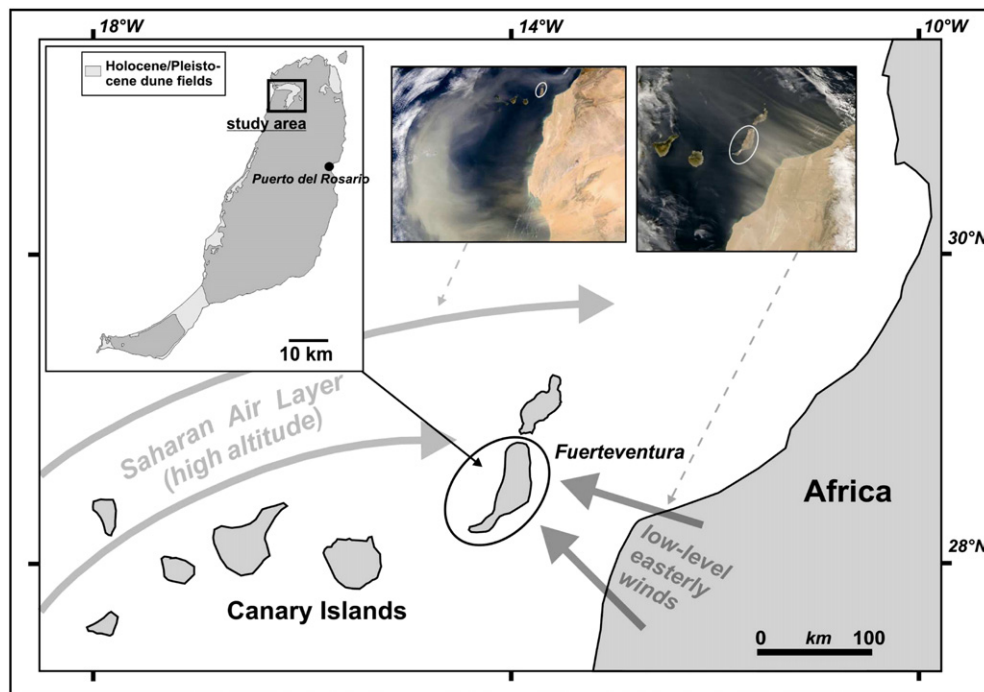


Fig. 2. Location of Fuerteventura off the coast of NW-Africa with indication of dune fields (adapted after Rothe, 1996). Main dust-bringing winds (Saharan Air Layer and low-level dust loaded eastern winds) are shown with arrows, and further illustrated by appropriate satellite-images where Fuerteventura is indicated with white ellipses (source: NASA, 1997).



Photo 1: Overview of the western part of the Melián section. Almost all layers are strongly reworked.



Photo 2: Eastern part of the Melián section. Layers are dipping in northern direction. Basaltic basement in front.



Photo 3: Costilla section showing the dune sand-paleosol sequence



Photo 4: Lajares III section. Note the remnants of the pedogenetic CaCO₃-crust on top of the sand deposits, covered by a colluvial layer.

Fig. 3. Site photos. Photo 1: Overview of the western part of the Melián section. Almost all layers are strongly reworked. Photo 2: Eastern part of the Melián section. Layers are dipping in northern direction. Basaltic basement in front. Photo 3: Costilla section showing the dune sand-paleosol sequence. Photo 4: Lajares III section. Note the remnants of the pedogenetic CaCO₃-crust on top of the sand deposits, covered by a colluvial layer.

stratigraphic and chronological context is critical for future studies that aim to investigate the biotic and climatic evolution during the Quaternary in the study region. Finally, this paper presents a broad discussion on soil formation processes and their major controlling factors.

2. Geographical setting

The Canary Islands are a volcanic archipelago situated off the Northwest African coast in the subtropical northeast Atlantic (Fig. 2). During most of the year the islands are under the influence of trade winds. Sparse precipitation is brought during winter by westerly cyclones occasionally following southern tracks and breaking the trade wind air layer over the islands.

On the orographically higher central and western islands, this kind of rainfall is supplemented by humidity from rising trade wind air (Rothe, 1996). Saharan dust is transported towards the Canary Islands mainly through three main routes, and consequently it may come from different sources. One contemporary dust pathway to the eastern Canary Islands is connected to easterly winds at low altitudes (0.5–1.5 km, Muhs, 2013) resulting from a pressure gradient between the northwestern Sahara (high pressure) and the Atlantic Sea southwest of the Canary Islands (relatively lower pressure). It is assumed that the main Saharan dust sources are the foothills of the Atlas Mountains and the Moroccan and Mauritanian coastal region (Stuut et al., 2005).

During the boreal winter, dust is brought by low-level continental African trade winds (branches of the Harmattan, southern pathway)

that block Atlantic cyclones moving along more southern tracks (Criado and Dorta, 2003). This configuration pushes the dust back to the Canary Islands by a deflected branch with dust loads at altitudes below 2 km (Muhs, 2013).

During summer, dust is transported to latitudes even farther north from the Canary Islands by the northern branch of the high altitude Saharan Air Layer (SAL). The material is transported at relatively high altitudes (up to 7 km; Muhs, 2013) and sinks into the lower atmosphere to reach the Canary Islands. A part of this SAL-dust is finally brought to the islands by the NE trade winds (Koopmann, 1981; Bozzano et al., 2002). The dust is deposited either in dry or wet form (Criado and Dorta, 2003; Menéndez et al., 2007).

Different generations of volcanoes with ages encompassing the entire Pleistocene form the volcanic bedrock of Northern Fuerteventura (Meco et al., 2008). Sand delivered from the shelf of the island, mainly composed by crushed shell fragments, was trapped in depressions and on the windward slopes of volcanic cones, where climbing dunes were formed. Subsequently, fluvial and colluvial processes reworked the eolian deposits and formed vast calcareous sand layers in the toe slope position of the volcanoes.

For the studied sand pits, we assume a prevailing sequence of geomorphic processes during the late Pleistocene that is characterized by an interaction such as sand accumulation, soil formation and erosion, and deposition of sand- and soil-derived sediments. Presently, the entire sequence is formed by remnants of sand dunes (as a rule only the lowermost part of the dune is preserved, whereas the upper part was

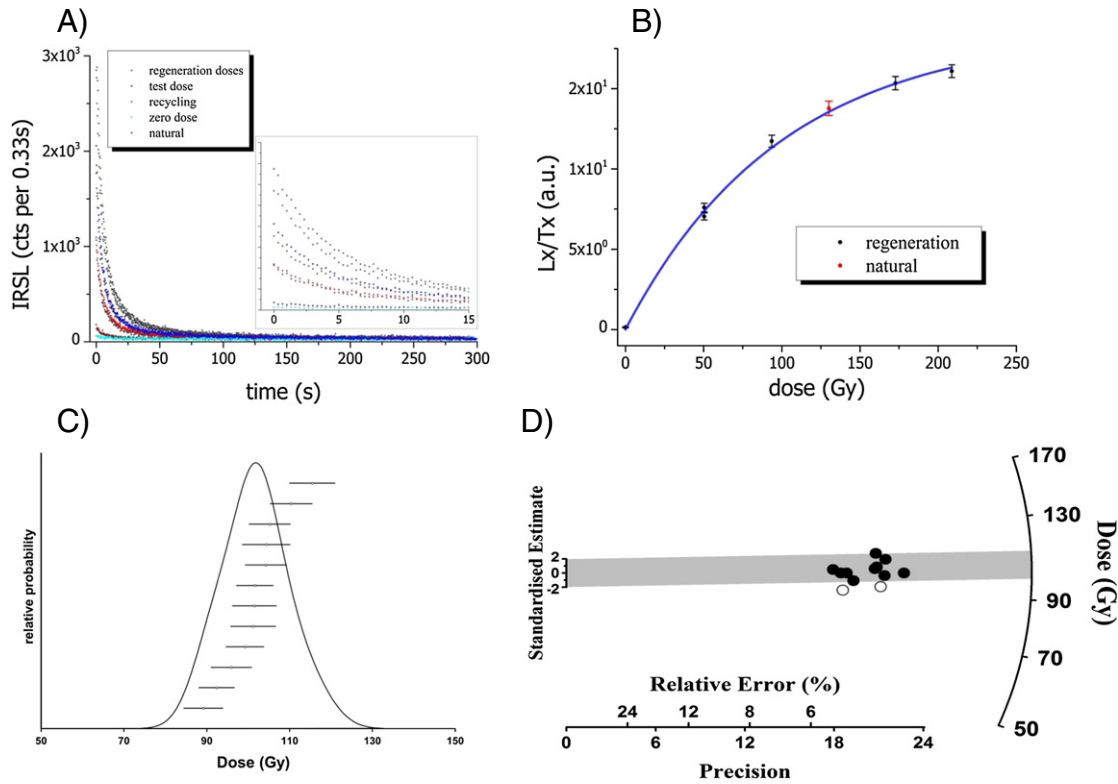


Fig. 4. Exemplary IRSL data for randomly chosen sample BT1089. A) IRSL curves from one aliquot, with the inset enlarged for the first 15 s of IR-stimulation (data not normalized). B) IRSL growth curve of the same aliquot. C) Relative probability and D) radial plot of equivalent doses of the 12 (out of 12) aliquots measured, showing an overdispersion of 4.7%.

eroded), reworked sand, sandy soil sediments and soils that were formed in situ (see Fig. 3). Erosional unconformities are visible in between.

Our own field observations show that Holocene morphodynamics point to the formation of small nebkha dunes in the study area that in some places cover the sand-paleosol sequences. Furthermore, the Holocene is characterized by weak soil formation (entisols) and the deposition of colluvial material on toe-slope positions.

Quaternary dune sand-paleosol sequences have never been described in detail from Northern Fuerteventura. Published studies (Damnati et al., 1996; Bouab and Lamothe, 1997; Ortiz et al., 2006; Meco et al., 2008; Gutiérrez-Elorza et al., 2013) have focused on age estimations of sediments regardless of their genesis (eolian, colluvial) and do not generally consider soil formation features.

3. Methods

3.1. Fieldwork

During two fieldtrips, four sandpits of several hundred meters in length (Fig. 3) were studied in detail to elucidate a much-needed robust stratigraphy. All eolian sequences were studied and analyzed, working at least on 4 quarry walls to establish a representative stratigraphic profile of every pit. Four representative sequences are presented in this paper (Figs. 5–8, see also Fig. 9) to illustrate a spatially broader stratigraphic context. The profiles of the four target pits were stratigraphically combined thereafter.

3.2. Analyses of soils and sediments

Geochemical analyses were conducted to support the stratigraphic interpretations from the fieldwork. For 47 samples standard analyses such as grain size distribution, CaCO₃-content and organic carbon as

well as some basic element determinations (see Figs. 5–8) were performed.

Geochemical analyses and grain size distributions were determined in the laboratory of the Department of Physical Geography at the Technische Universität Dresden, Germany. Grain size analyses were conducted using the pipette analysis and wet sieve techniques (Schlichting et al., 1995) after dispersion in sodium pyrophosphate.

Soil organic matter was measured via suspension and catalytic oxidation (TOC-VCPN/DIN ISO 16904). Carbonate content was determined by measuring the carbon dioxide gas volume after adding hydrochloric acid in a Scheibler apparatus (Zielhofer et al., 2009). Pedogenic iron content (Fed) was measured after dithionite extraction using atomic adsorption spectrometry (Schlichting et al., 1995; Zielhofer et al., 2009). The content of basic chemical elements such as Fe_{total}, Ca, Al, K, Mg, Na, Sr and Zn was determined after pressure digestion with concentrated nitric and hydrofluoric acid, using atomic adsorption spectrometry.

Terrestrial gastropod samples were retrieved only from paleosols because dune sands were poor in shells. Soils and sediments were sampled according to visible color and texture variations in the field. Unclear transitions of paleosols into sediments were sampled and studied in greater detail. In case of very thick sand layers, up to three samples were taken from each layer.

3.3. Environmental magnetism

Magnetic susceptibility and frequency-dependent magnetic susceptibility were measured in the laboratory of the Institute of Geography, University of Leipzig (Germany) using a Bartington MS3 magnetic susceptibility meter, equipped with an MS2B dual frequency sensor. Before measurement the material was gently ground, densely packed into plastic boxes, and the volume magnetic susceptibility κ was measured at low frequency (0.465 kHz, $\kappa_{(LF)}$) and high (4.65 kHz, $\kappa_{(HF)}$) frequency. By normalizing the low-frequency measurement

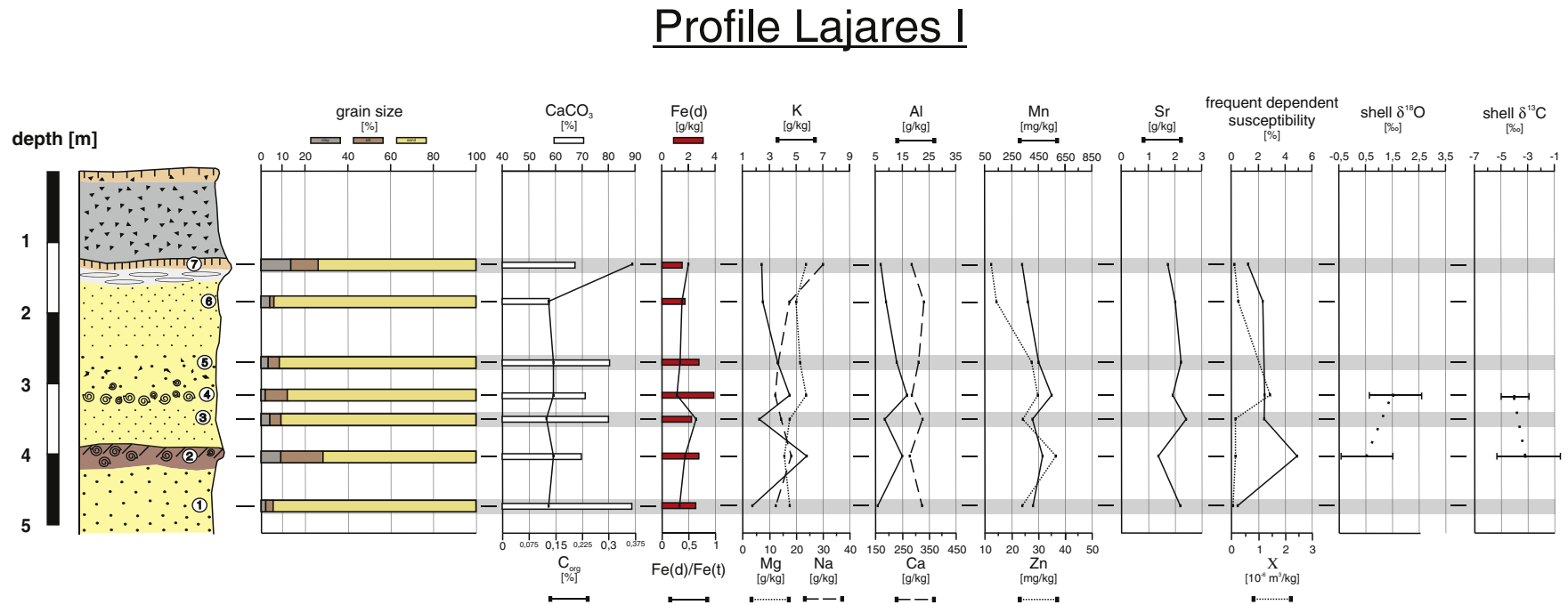


Fig. 5. Lajares I-section showing on top a weak soil in a colluvial layer (no geochemical data) and a weak soil (sample 7) over a solid pedogenetic CaCO₃-crust. Sample 4 represents a truncated soil (mollusk line) that is supported by the geochemical data (Fe_d, K, Al, Mn). At a depth of about 4 m a reddish soil (sample 2) marks the end of a phase of sand accumulation (sample 1). Key to the symbols see Fig. 10.

Profile Lajares III

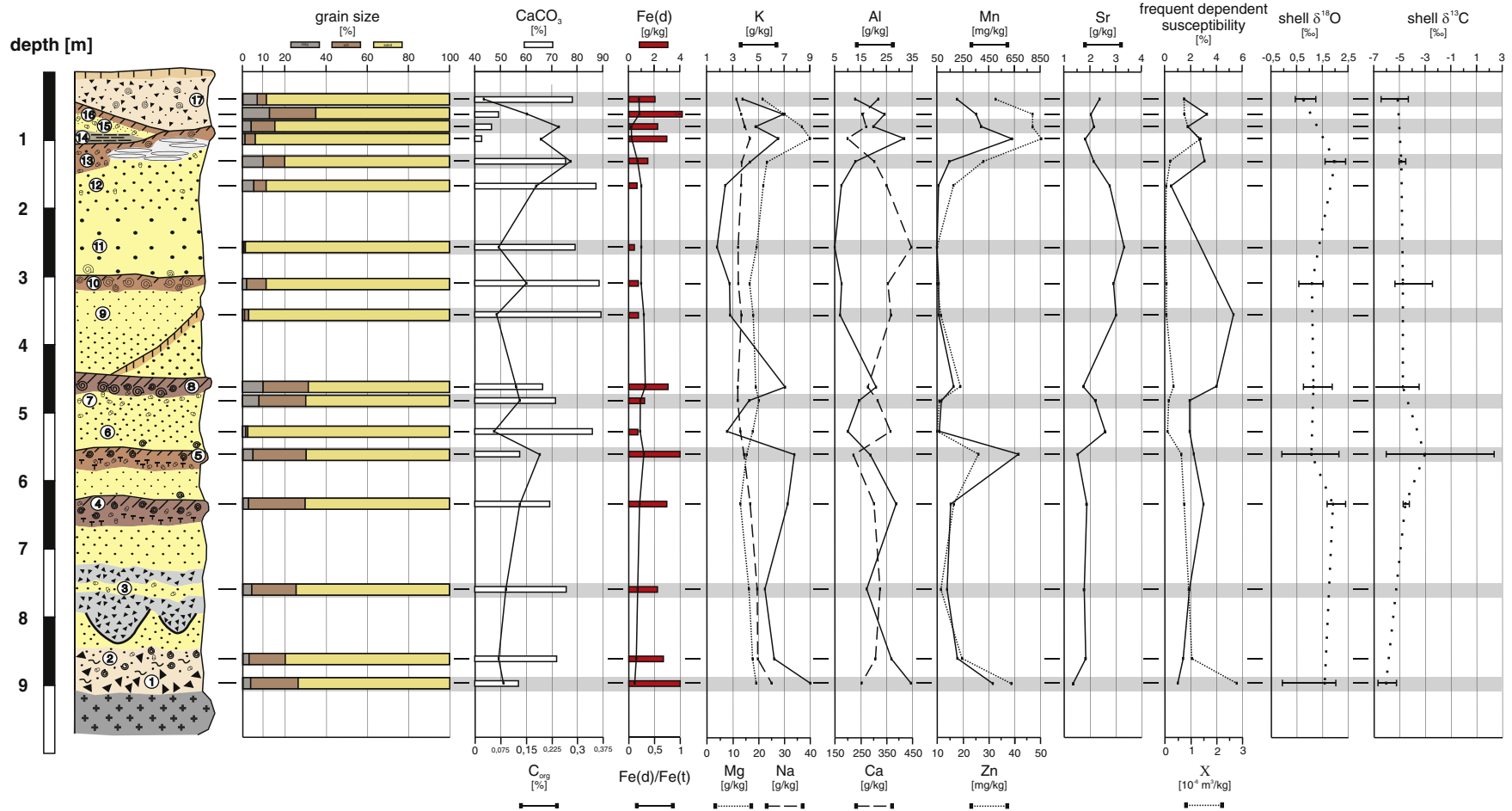


Fig. 6. Lajares III-section with identical features in the upper part compared to all other sequences. The middle part of the section seems to be more complete (from sample 11 to 7) than in other sections. The upper soil in the middle part (sample 10) obviously is of less intensity showing high CaCO₃-values and low K- and Al-content. Granulometric data support this assumption. Sample 14 represents a reworked volcanic ash layer with highest Mg, Mn and Zn-content. Key to the symbols, see Fig. 10.

Profile Melian

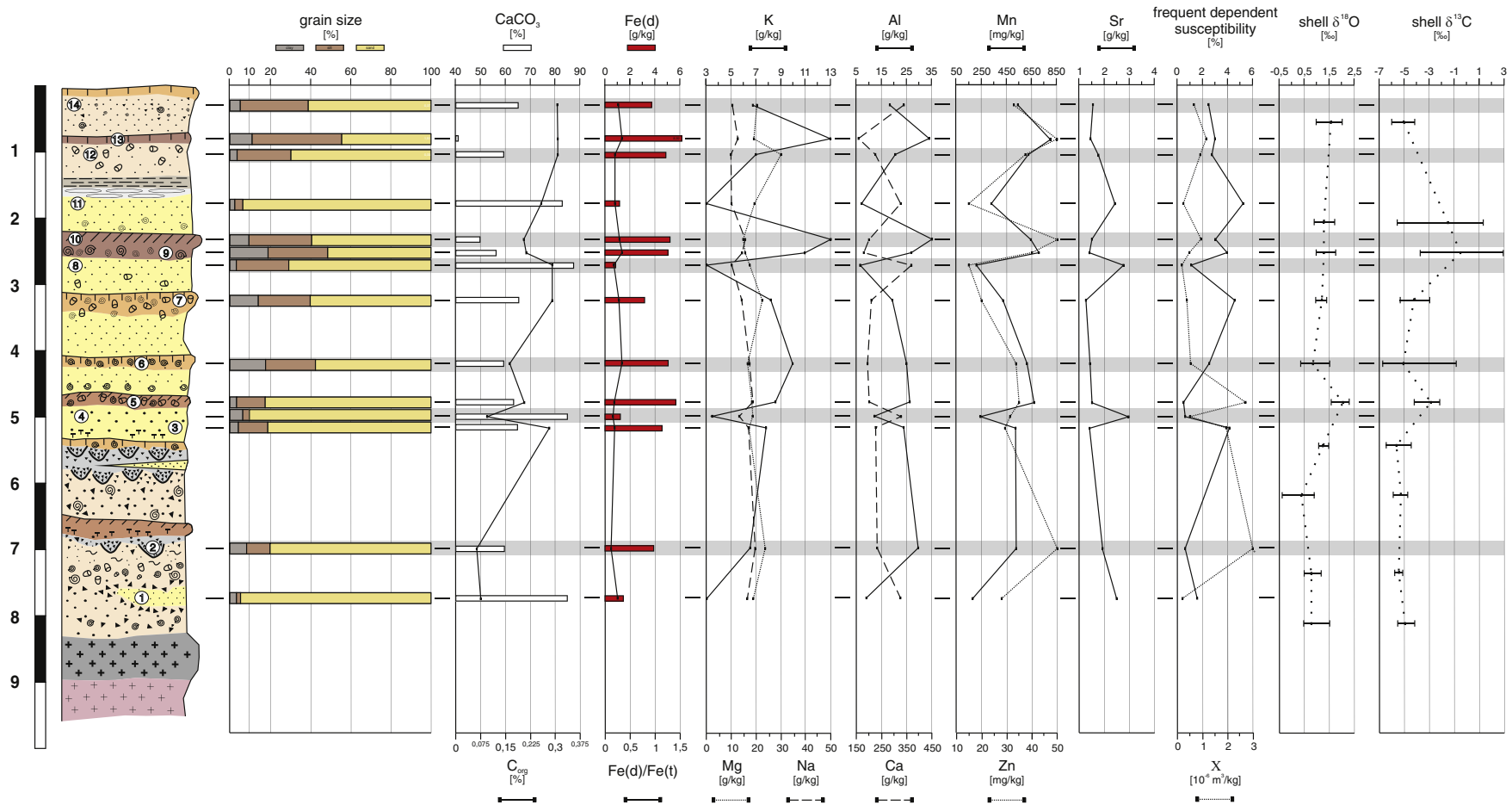


Fig. 7. In the Melián section the stratigraphic lower part (sample 7 to 3) is characterized by three soil formation periods (sample 7, 6, 5) all being older than MIS 5. We assume soil-forming periods within the penultimate glacial. The soil (sample 10) seems to be polyphasic with long exposure times. This is supported by the data of soil formation (high Fe(d)-, high K- and high Al-content) and the incorporation of volcanic ash (very high Zn- and Mn-content). The lower part of the Melián section shows several erosion events (phases?) as seen in subsequent refilled small gullies. Key to the symbols see Fig. 10.

Profile Costilla

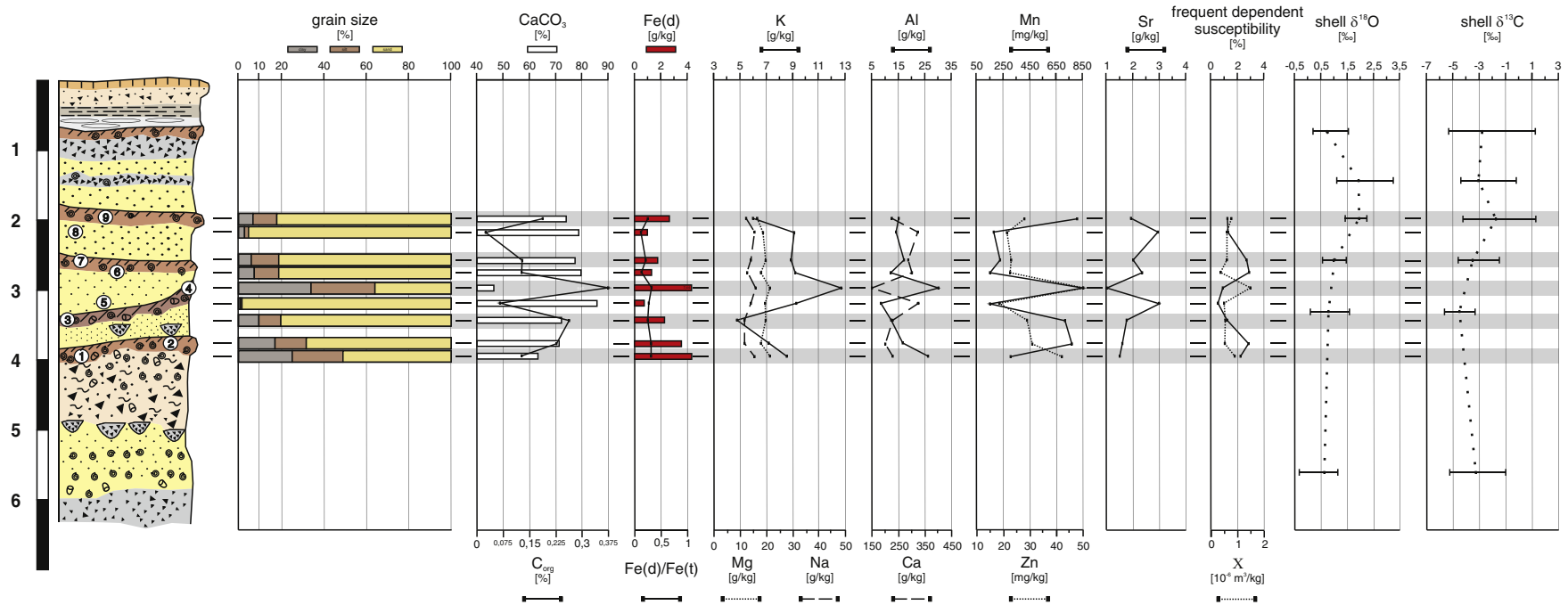


Fig. 8. Collected data from the Costilla section. The uppermost part and lowermost part are of less relevance for this study that aims to correlate soil and sand units. Therefore geochemical analyses were conducted on sand paleosol sequences (sample 1–9) showing the strongest soil (sample 4) of all studied pits. Key to the symbols see Fig. 10.

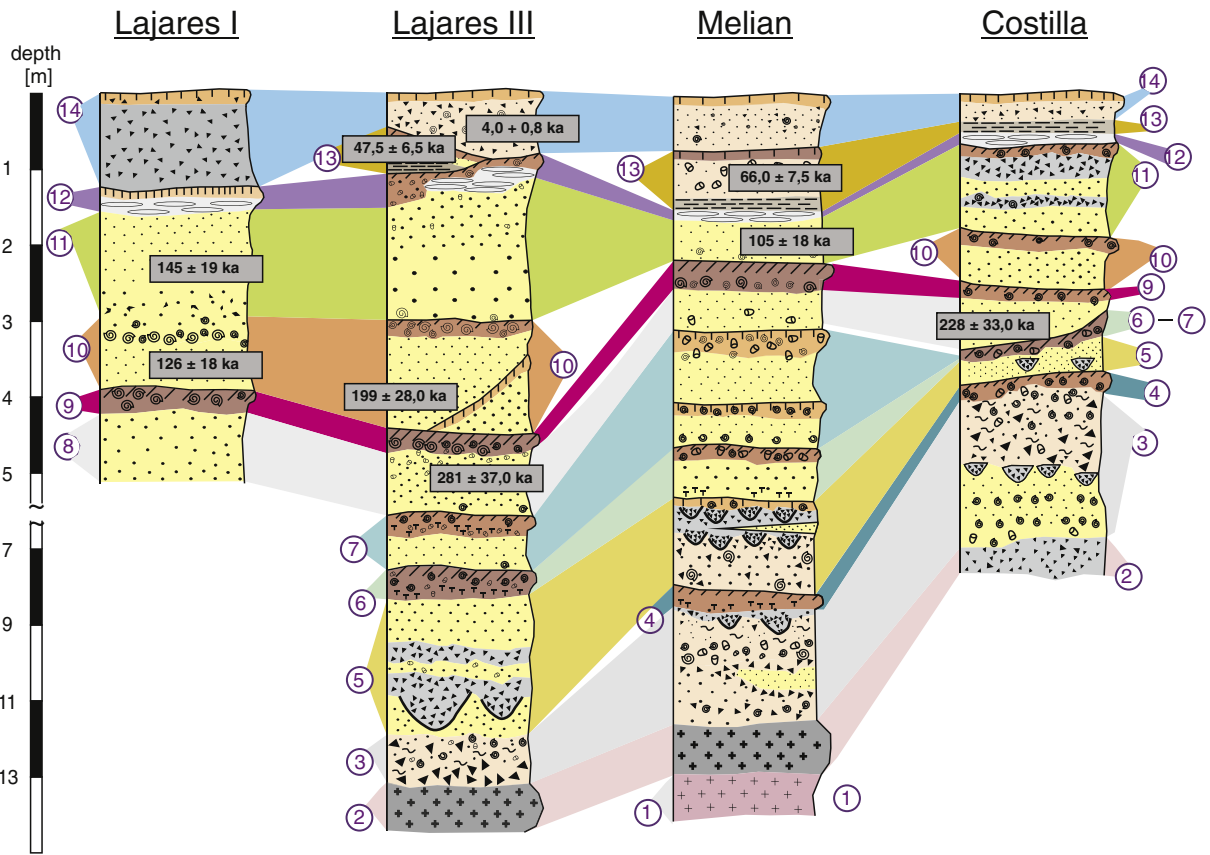


Fig. 9. Stratigraphical and chronological correlation of dune sand-paleosol-sequences in Fuerteventura (sedimentation units are marked by numbered circles and colored bands). Key to the symbols see Fig. 10.

($K_{(LF)}$) with the mass of a sample, we obtained mass-specific magnetic susceptibility χ_{lf} , subsequently termed χ . Frequency-dependent magnetic susceptibility χ^{fd} (in %) was calculated with the equation (e.g. Dearing, 1999):

$$\chi^{fd} = (K_{(LF)} - K_{(HF)}) / K_{(LF)} * 100.$$

3.4. Stable isotopes of terrestrial gastropod shells

Terrestrial gastropod shells were measured in the Department of Earth and Environmental Sciences (University of Kentucky, USA). Adult gastropod shells of the species *Theba geminata* (Gastropoda: Helicidae) were selected for oxygen and carbon isotopic analysis

because it is the dominant taxon throughout the Quaternary in Fuerteventura. A total of 104 shells recovered from 25 stratigraphic horizons (paleosols) of the studied four pits were analyzed isotopically. Between 3 and 5 shells per soil horizon were measured to obtain a representative average isotopic value for each paleosol (Yanes et al., 2011). Whole-shell analyses were preferred over intra-shell measurements because we aimed to deduce average (dominant) paleoenvironmental conditions rather than seasonal patterns. Each entire shell was cleaned with DI water and ultrasonication to remove detrital contaminants. Oven-dried entire shells were finely ground by hand using an agate mortar and pestle. Shell powder was then treated with 3% hydrogen peroxide for 12 h to remove humic contaminants, subsequently rinsed three times with DI water, and finally dried at 40 °C overnight. About 150 µg of carbonate was placed in a 6 ml Exetainer™ vial that was

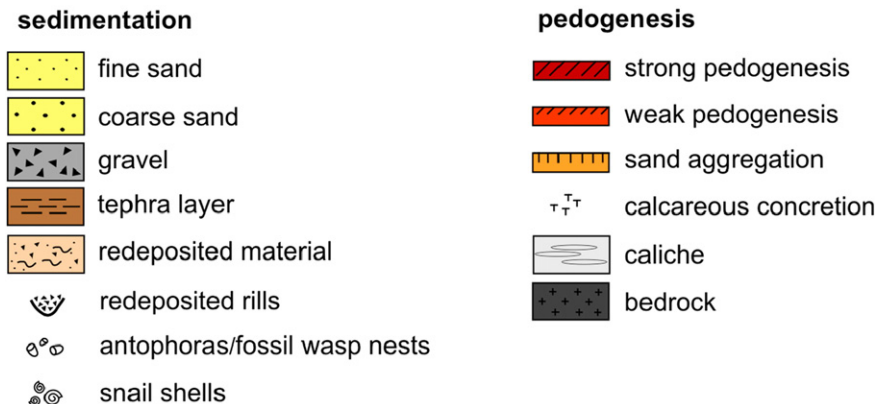


Fig. 10. Key to the symbols for Figs. 5–9.

flushed with helium. The carbonate was converted to CO₂ (gas) with 0.1 ml of 100% H₃PO₄ at 25 °C during 24 h. The CO₂ was analyzed in a Gas Bench II peripheral device connected to the isotope ratio mass spectrometer (IRMS) Finnigan Delta plus XP. Analytical uncertainty was ± 0.1‰, based on in-house and international (NBS-19) standards. All stable isotope data are reported in δ notation relative to the international standard Pee Dee Belemnite (PDB). The δ value is defined as:

$$\delta_{13C} \text{ or } \delta_{18O} = [(R_{\text{sample}}/R_{\text{standard}}) - 1] \times 1000(\text{‰})$$

where R = ¹³C/¹²C or ¹⁸O/¹⁶O.

3.4.1. Luminescence dating

Samples for luminescence dating were either extracted by steel cylinders hammered horizontally into the sediment, or by cutting blocks of solidified sediments, which were wrapped in aluminum foil and light-tight plastic bags. The samples were processed in the luminescence laboratory of the Geomorphology Chair at the University of Bayreuth under subdued red diode light (640 ± 20 nm). The light-exposed outer rim (2–4 cm) of the samples was removed prior to sample preparation. The coarse and middle grain fractions (90–200 μm, 40–63 μm) were separated from the finer fraction (<40 μm) by wet sieving. The fine grain fraction 4–11 μm was obtained by settling in Atterberg cylinders following Stokes' law. All fractions were decalcified in 10% HCl and organic matter was removed in 10% H₂O₂.

Attempts to obtain a sufficient amount of quartz separates for OSL dating from the mostly calcareous dune sands by applying heavy liquid separation in diluted Li-polytungstate ($\sigma = 2.75 \text{ g/cm}^3$) and subsequent etching in concentrated HF (coarse grains) and H₂SiF₆ (fine grain fraction, cf. Fuchs et al., 2005), respectively, failed. Consequently, only polymineral fine grain IRSL-dating was possible for these sediments. Aliquots were prepared by pipetting of a suspension in demineralized water (1.2 mg/200 μl) on 9.6 mm diameter aluminum discs so that fine grains settled on each disc during evaporation. Due to limited amounts of fine grain material and machine time, a SAR protocol was applied, which is based on results from Huot and Lamothe (2003), Preusser (2003) and Rother et al. (2010). IRSL measurements were executed on a Risø DA15 automated reader at 90% diode power for 300 s at 125 °C. The IRSL detection was restricted to the blue wavelength band (Croma D410, transmission 410 ± 20 nm) in order to minimize the potential fading problem of feldspar (Lang and Wagner, 1997). The absence of significant fading for this blue emission recorded after strong preheat and cutheat was shown in several studies (e.g. Preusser, 2003; Rother et al., 2010). Identical conditions (Huot and Lamothe, 2003) of 270 °C for 120 s (Zöller, 1995; Rother et al., 2010) were employed for the preheat and cutheat of the SAR protocol. A resting period of 20 min was allowed between beta dosing and IRSL readout. Possible anomalous fading was assumed to be minimized and likely to be non-significant for this protocol following the results of Rother et al. (2010) and Preusser (2003). The limited availability of fine grain material and machine time so far has inhibited a systematic determination of anomalous fading. Therefore the obtained IRSL ages have to be regarded as minimum ages. But given the absence of IRSL age underestimation for most samples from Lanzarote with a similar detection wavelength band (Suchodoletz et al., 2008) we presume as such for our samples.

After initial tests with a regeneration dose of ca. 0.5 of the equivalent dose (ED), the regeneration doses were set to approximately 0.4ED, 0.8ED, 1.2ED, 1.6ED, 0, and 0.4ED.

The IRSL data of the first 10 s (subtracted background determined by the last 34 s) was analyzed with the Analyst software for exponential fitting of the dose response (Fig. 4). A measurement uncertainty of 1.5% and 1000 Monte Carlo repeats were employed for ED determination (Duller, 2007). All data not meeting the maximum deviation of the recycling point of ± 0.1 within unity (recycling point incorporated in fitting), test dose errors and recuperation larger than 10% and 4%,

respectively, and a signal lower than 3 times the background, were all rejected. Dose-rates were derived from thick source alpha-counting (U, Th) and ICP-MS (K) using conversion factors given by Guerin et al. (2011). Cosmic dose-rates were calculated after Barbouti and Rastin (1983). Interstitial water content representative for the burial period was taken as 10 ± 5%, and an a-value of 0.07 ± 0.02 was adopted from Preusser et al. (2008), which is slightly larger than a-values for loess-like sediments on Lanzarote Island determined by Suchodoletz et al. (2008).

4. Results

Each individual sand pit is described separately in this section and illustrated in Figs. 5–8.

The analyzed samples from each profile were labeled using sequential numbers (from sample 1 to sample n + 1) starting at the respectively lowest (oldest) level. The general overview and stratigraphic correlation between profiles is shown in Fig. 9 and combines sedimentary units. Note that unit numbers in Fig. 9 do not correspond to sample numbers in Figs. 5–8.

Sedimentary units in Fig. 9 represent either a cycle of sand deposition and subsequent soil formation, or a sequence of sand deposition and following erosion. The next unit then starts with a new depositional episode.

4.1. Stratigraphy

4.1.1. Lajares I (Fig. 5)

Site 1 is called "Lajares I" and is situated about 2 km east of the village of Lajares (N 28° 40' 33.00", W 13° 55' 14.50"; altitude 80 m a.s.l.). It is the smallest pit and we were not able to expose levels deeper than 5 m. The sandy strata are dipping northwards following the morphology of the basaltic bedrock. The sequence shows features of soil formation such as rubefaction, brunification and partly decalcification (Fig. 5), observable in all other profiles as well. Some nebkha dunes of young age were formed on top. The uppermost part of the sequence shows a colluvial layer containing sand and volcanic lapilli. A weak aridisol was formed in this material. Below the colluvial layer a very weak soil (sample 7) was formed on top of a strong calcium carbonate crust. However, this pedogenetic crust does not belong to the weak soil (sample 7) because its formation would have required a strong decalcification of the material above. The soil that had formed the crust must subsequently have been eroded. This calcium carbonate crust depicts the first clear feature of a strong pedogenesis process under free-draining conditions and is observed in all other pits.

The parent material is coarse sand with some volcanic ash mixed in. A small (~6–9 mm) gastropod shell assemblage is concentrated at about 3 m depth (sample 4). The corresponding soil has been eroded so that only the lowest part of a former soil is preserved. This shell concentration is formed almost entirely by *T. geminata* (sub-adult and juvenile ontogenetic stages) specimens and clearly separates a coarse sand layer with high content of ash above (sample 5) from a fine sand layer with poor ash content below (sample 3). This is the next clear feature that is found in all other profiles as well. A strong reddish soil is developed on top of a homogenous sand layer at 4 m depth. Due to its distinctive characteristics, such as a strong red color, this marker soil (sample 2) has the highest content of pedogenic iron compared to all other soils in this study and a high redness rating value (H[†] x Chroma/Value) after Torrent et al., 1980.

4.1.2. Lajares III (Fig. 6)

The Lajares III site is an extensive sand quarry situated south of the Lajares village (N 28° 39' 53.00", W 13° 56' 13.00", altitude 93 m a.s.l.)

[†] H = 12.5 for Munsell hue of 7.5R; 10 for 10R; 7.5 for 2.5YR; 5 for 5YR; 2.5 for 7.5YR and 0 for 10YR.

with strata dipping in northward direction, as for Lajares I. The uppermost part of the section is comparable to Lajares I, with a firm crust of CaCO_3 found below a colluvial ash layer. The soil horizon (sample 10) is similar to the eroded soil of Lajares I (sample 4), characterized by a distinctive narrow concentration of small shells. Lajares III also exhibits a weakly developed soil with a distinctive sub-adult-juvenile (small-size) *T. geminata* concentration, which separates the coarse sand above (sample 11) from the fine sand (sample 9) beneath. A weak soil was formed between these two depositional phases. The reddish marker soil in Lajares I (sample 2) is also well developed in Lajares III (sample 8), with a relatively high redness rating of 1.43 compared to the soils above (0.63). Below this marker horizon that is developed on a sand layer (sample 7, 6), a soil or soil sediment with a high content of volcanic ash (sample 5) appears. The deepest part of the section shows remobilisation of sand and lapilli with small gullies infilled with lapilli and coarser stony fragments of basaltic origin. We observed here two depositional layers of chaotic composition (sand, lapilli, coarse basaltic fragments), indicative of two erosive phases. Above these features, a soil was formed on top of one of the earliest dune generations (sample 4).

4.1.3. Melián (Fig. 7)

The Melián section is the largest investigated quarry, situated west of the village of Lajares (N 28° 40' 22.00" and W 13° 57' 10.00", altitude 90 m a.s.l.). The pit is about 500 m long and 250 m wide, and the deepest point reaches about 25 m below the present-day ground surface. The uppermost part of the section is characterized by two colluvial layers separated by a weak soil (sample 13).

The remains of a pedogenetic CaCO_3 -crust are preserved under a ubiquitous ash layer (also present in Lajares III, sample 14) that was reworked by alluvial processes. A very well developed soil (sample 10) is observed at about 2.5 m depth. This soil matches with our "marker soil" present in all other sequences, assuming a hiatus of sand delivery resulting in a longer process of soil formation. Below this soil there is a successive alternation of dune sand-paleosol levels. The deeper part of the sequence below 5.5 m is characterized by two erosional phases with rill erosion phenomena. These rills are infilled with basaltic gravels. In between, at a depth of 5.8 m, remnants of a dune generation were observed. Another soil developed in a colluvial layer below, which is incised by small rills (sample 2). The entire reworked colluvial material below a depth of 5.5 m is composed by sandy and silty material with a high content of lapilli, gastropod shells and arthropod nests. The first dune sand generation developed at about 8 m depth (sample 1). The bottom of the sequence shows a solid lava flow that covers a very strongly altered reddish and saprolitic lava.

4.1.4. Costilla (Fig. 8)

The Costilla sequence is the northernmost pit, situated at N 28° 41' 17.00" and W 13° 58' 13.00", at an altitude of 55 m (a.s.l.). A colluvial horizon is present on the top of this sequence, in which a very weak soil was formed. An ash layer, reworked by alluvial processes, is present immediately underneath (cf. Lajares III, sample 14; Melián, below sample 12). A pedogenetic CaCO_3 -crust is present right below this ash layer. As in the other pits, the respective soil material was eroded. Sandy and lapilli-rich layers alternate at a depth between 1 and 2 m. This episode is followed by a weak soil formation phase on top of the uppermost lapilli-rich layer.

Geochemical analyses were conducted on the central part of the sequence (from 2 to 4 m) to understand the transitional process from dune sands to paleosols.

The strongest soil formation, observed between 3.5 and 3 m of depth (sample 4), is characterized by a high content of pedogenetic iron pointing to a long-lasting period of soil formation. The overlying soil (sample 7) corresponds to our marker soil. The soil at a depth of about 4 m (sample 1 and 2) is developed on top of a colluvial layer that

contains a mixture of soil sediments, lapilli, sand and fragments of gastropods and arthropod nests. This colluvial episode seems to have started with an intensive erosion phase, as documented by the presence of rills filled with coarse-lapilli and basaltic fragments, similar to the above-described sections. Dune sands containing two distinct concentrations of gastropod shells developed right below this feature, which points to a temporary standstill in sand supply. The lowest part of the section shows a colluvial layer that mainly contains lapilli and basaltic fragments.

4.1.5. Composite stratigraphy of all sections

The correlation of the sections drawn from four sand quarries in the northwestern part of Fuerteventura Island is based on sedimentary units and provides the following composite stratigraphy (Fig. 9): On top of all sections a colluvial layer of varying thickness is developed. The first stratigraphic marker layer is an ash layer relocated over short distances (Lajares III, unit 13). Below this ash layer a CaCO_3 -horizon (crust) was formed during a period of soil formation (unit 12). The corresponding soil has been eroded so that the Cc-horizon was exposed. However, soil formation took place under conditions of free drainage as all settings are sandy with good infiltration conditions. In our interpretation, even if the corresponding soil was eroded the solid pedogenetic CaCO_3 -crust witnesses long-lasting conditions that were favorable for soil formation.

The underlying stratigraphic marker is the change from a coarse sandy layer containing dark volcanic ash grains (Fig. 9, unit 11) to an underlying fine sandy layer almost free of volcanic ash (Fig. 9, unit 10). The boundary between these two layers is marked by a concentration of small (sub-adult and juvenile) snails (*T. geminata*). This transition is found in three (Lajares I, Lajares III and Melián) out of the four sections. The subjacent marker horizon is an intensively developed soil (Fig. 9; unit 9) that is rich in terrestrial gastropods with variable shell sizes, ontogenetic stages and relatively high species diversity. Levels developed below this episode differed significantly between pits due to either sand-supply pause or erosion. In particular, units 6 and 7 (Fig. 9) exhibit very different preservation conditions. In the Melián section, three soils of different intensity were formed, whereas in the Costilla section these units converge and one strong soil (highest Al, K and Fed-contents) was formed (polyphasic?) during a longer timespan (compared to sections Lajares III and Melián).

The lowest part in all sections exhibits at least two marked erosion episodes with incised rills and small gullies in sandy and/or colluvial material. Those rills are infilled with coarse material consisting of lapilli or basaltic rock fragments.

4.2. Analytical results

Results of grain size analyses show higher clay and silt content in soils and soil sediments than in dune sands. In sand layers the content of silt and clay is below 10%. An interesting feature is the relatively large content of silt (~20–25%) in the sediment layer below the marker soil (Lajares III, sample 7; Melián, sample 8). It is almost as high as in soils, whereas other sediment layers with comparable features contain less than 10% of silt. Thus, grain size results are an additional feature for the stratigraphic correlation between these layers. The origin of the silt is still an open question. Higher silt content in soils may be either a feature of in situ soil formation by weathering of fine sand or a feature of increased Saharan dust supply, while sand supply decreased.

CaCO_3 -content is a good marker to detect soil formation intensity (Duchaufour, 1982; Zielhofer et al., 2009). All analyzed soils in this study show a relatively low content in CaCO_3 that suggests a decalcification of the dune sands having primary CaCO_3 -contents of about 80%. According to their geochemical characteristics (i.e., low content of CaCO_3 , pedogenic iron, and K and Al, together with a high redness value of 1.43) we assume that the marker soil in Melián (sample 10)

and Costilla (sample 4) was formed during a long timespan associated with long-lasting exposure times. These features are not clearly developed in the marker soil of Lajares I and Lajares III sections. In general, the tendency of decreasing CaCO₃-content is obvious in all soils and soil sediments.

The content of pedogenetic iron (Fed) is generally high in soils and soil sediments. The marker soil (sample 8) in the Lajares III section shows a relatively high content of the pedogenic iron (Fed)/total iron (Fet) ratio, pointing to a significant alteration of Fet into Fed. This supports the idea of intensive soil formation. The content of total iron (Fet), however, is also related to the input of volcanic ash, showing the highest value in the volcanic ash layer itself (Lajares III, sample 14) and relatively high values in soils and soil sediments. It is assumed that the soils were exposed to the atmosphere for a long time, allowing for the incorporation of all tephra events that happened on the eastern Canary Islands during exposure time. The longer the surface was exposed the higher the tephra input was, as can be seen by the magnetic susceptibility of the marker soil that is strongly dominated by volcanic particles. The soil sediments, in turn, are reworked and redeposited soils so that their high iron content is inherited.

Caquineau et al. (1998) reported a high content of both kaolinite and illite in Saharan dust, and Suchodoletz et al. (2008) correlated Al content in marine cores close to the Canary Islands and kaolinite content. Furthermore, neoformation of kaolinite is almost impossible in settings on Fuerteventura, where a relatively high content of exchangeable cations (Ca, Mg, K, Na) in soils and sand deposits precludes the formation of kaolinite. Accordingly, due to the regular input of Saharan dust on Fuerteventura, K- and Al-contents in our sequences are mostly considered as allochthonous elements that were transported with Saharan dust as CMA (clay-mineral-aggregates; Smalley et al., 2013) to Fuerteventura. Therefore, both elements are generally strongly correlated, as can be seen in Figs. 5–8. For cases lacking such correlation (e.g. Melián, sample 6 to 5 in the middle part of the section; Lajares III, sample 5 to 4 between 6.5 and 5.5 m) we assume either a possible change of the dust source in West Africa, or a higher input of local volcanic material, showing different proportions of both elements.

Mn- and Zn-content is related to volcanic ash input, showing the highest peaks in the ash layer of Lajares III (sample 14). Soils and soil sediments show similar features in all profiles (e.g., Lajares I: sample 4 and 2; Melián: sample 10; Costilla: sample 9 and 4) due to enrichment of tephra input during exposure times (soil formation).

4.3. Chronology

As all quoted IRSL ages presented here (Fig. 9; Table 1) may have suffered from uncorrected anomalous fading, these ages should be formally regarded as minimum ages.

Table 1
IRSL-dating, analytical results and ages.

Laboratory code	Field code	U (ppm)	Th (ppm)	K (%)	Dose rate (Gy/ka)	ED (Gy)	Age (ka)
<i>Lajares I</i>							
BT 1088	Laj I-1	1.41	0.56	0.15	0.89	129 ± 9.0	145 ± 19
BT 1089	Laj I-3	1.48	0.34	0.08	0.81	102 ± 7.2	126 ± 18
<i>Lajares III</i>							
BT 1093	Laj III-1	1.37	1.35	0.23	1.06	4.22	4.0 ± 0.8
BT 1095	Laj III-3	1.23	1.39	0.31	1.07	50.9 ± 5.6	47.5 ± 6.5
BT 1096	Laj III-4	1.41	0.48	0.07	0.75	150 ± 6.5	199 ± 28
BT 1097	Laj III-2	2.15	3.71	0.62	1.87	525 ± 44	281 ± 37
<i>Melián</i>							
BT 1090	Laj II-1	1.25	2.01	0.45	1.28	84.5 ± 5.8	66.0 ± 7.5
BT 1091	Laj II-2	1.25	0.64	0.12	0.81	85.3 ± 14	105 ± 18
<i>Costilla</i>							
BT 1101	ElRoque	1.31	0.33	0.08	0.68	155 ± 6.5	228 ± 33

The lowermost age from the section Lajares III (281 ± 37 ka) is the oldest luminescence age obtained so far for the Canary Islands. Due to the mostly calcareous lithology of the dune sands, our dose rates are considerably lower than those of loamy sediments dated on Lanzarote, allowing for a much older upper dating limit (cf. Suchodoletz et al., 2008).

The preliminary nine IRSL age estimates here are in consistent stratigraphic order and do not contradict our independently elaborated standard field stratigraphy for the past ca. 280 ka. The observed numerous erosional hiatuses and discordances require, however, a more detailed discussion and interpretation. The overall good correspondence between field stratigraphy and IRSL ages (including systematic uncertainties) suggests that the presented chronology here is credible. Moreover, the obtained ages of age-equivalent layers from different sections provided results that are consistent with the proposed stratigraphy. At Lajares III the youngest layer (4.0 ± 0.8 ka, BT 1093) overlies a partly truncated buried soil developed in a colluvial and aeolian layer dated to 47.5 ± 6.5 ka (BT 1095, unit 13), with a similar age obtained for unit 13 (66 ± 7.5 ka, BT 1090) in the Melián section. The eolianite (unit 11) yielded ages of 145 ± 19 ka at Lajares I (BT 1096) and 105 ± 18 ka (BT 1091) at Melián, respectively. Ages for aeolianite unit 10, including a partly truncated paleosol, range from 126 ± 18 ka (BT 1089) at Lajares I to 199 ± 28 ka (BT 1096) at Lajares III and 228 ± 33 ka (BT 1101) at Costilla, respectively. The single apparent age for unit 8 (281 ± 37 ka, BT 1097) at Lajares III supports the possibility that the exposed sections cover a time span of several hundred thousands of years, as is also suggested by U–Th and IRSL ages reported by Meco et al. (2008).

4.4. Environmental magnetism

Rather high values of mass-specific magnetic susceptibility (χ) of up to $3.3 \times 10^{-6} \text{ m}^3 \text{ kg}^{-1}$ demonstrate the dominance of volcanic material in the magnetic signal of the sequences.

Thus, in case of strong admixture of tephra particles into soils, the expected pedogenetic enhancement of χ_{fd} is hardly recognizable, as observed in the marker soil of Lajares III, Melián and Costilla. On the other hand, the admixture of formerly eroded soil material into dune sands is recognizable by relatively high values of χ_{fd} in such sand layers, as documented in sample 11 from Melián, whereas pure dune sand of shelf origin shows significantly lower values of χ_{fd} .

4.5. Stable isotope results

The stable isotope composition of fossil terrestrial gastropod aragonitic shells was measured to deduce the paleoenvironmental conditions during soil formation at various glacial intervals.

The isotopic results here consist of previously unreported data and they represent an extension of the study by Yanes et al. (2011). The carbon isotopic composition ($\delta_{13}\text{C}$) of fossil shells from northern Fuerteventura ranged from −6.9‰ to +3.0‰, whereas the oxygen isotope values ($\delta_{18}\text{O}$) ranged from −0.4‰ to +3.3‰. The shell $\delta_{13}\text{C}$ values inform us about the relative abundance of C₃ versus C₄ type plants, while the shell $\delta_{18}\text{O}$ values primarily depict humidity conditions (e.g., Yanes et al., 2008, 2009, 2011). Higher $\delta_{13}\text{C}$ values reflect higher abundance of C₄-type plants while lower values indicate an increase in C₃-type plants. An increase in C₄ plants may be linked to somewhat warmer/drier conditions or lower atmospheric CO₂ concentration (Yanes et al., 2011, 2013a,b). Broadly, higher shell $\delta_{18}\text{O}$ values depict somewhat drier conditions associated with lower relative humidity and/or higher rain $\delta_{18}\text{O}$ values whereas lower values point to wetter scenarios, i.e., higher relative humidity and/or lower rain $\delta_{18}\text{O}$ values. Isotopic data are described separately for every dune sand-paleosol-sequence.

4.5.1. Lajares I

The shell $\delta_{13}\text{C}$ values reveal negligible changes in the relative proportion of C₃/C₄ vegetation, but the $\delta_{18}\text{O}$ values point to wetter

conditions during the formation of the red marker soil (sample 2) than the soil above (sample 4) that formed during a shorter time span. Thus, snails suggest that the marker red soil (sample 2) was formed at times of higher moisture conditions than the horizon immediately above (sample 4).

4.5.2. Lajares III

In contrast to Lajares I, snail data from Lajares III indicate that moisture conditions and vegetation were comparable between samples 8 and 10. This finding suggests that soils on top of the unit 10 (Fig. 9) were formed under somewhat wetter environmental conditions in Lajares III than in Lajares I, while the marker soil (Fig. 9; unit 9) at both pits showed statistically equivalent isotopic data, pointing to similar moisture regimes. Shell $\delta_{18}\text{O}$ -values also indicate that sample 13 (Fig. 6; around 50 ka) was deposited during significantly drier conditions than preceding age-intervals. However, shell $\delta_{13}\text{C}$ values suggest that the C_3 – C_4 plant ratio remained comparable throughout all age-intervals of this pit.

4.5.3. Melián

The shell $\delta_{13}\text{C}$ values indicate a higher abundance of C_3 type plants in the lowest part of the section (unit 3–5, see Fig. 7) and a rise in C_4 type plants in samples 10 and 11 (Fig. 7). The $\delta_{18}\text{O}$ values suggest that humidity fluctuated throughout the section, pointing to wetter conditions during the formation of the oldest horizons (unit 3–5, see Fig. 9) and slightly drier conditions thereafter.

4.5.4. Costilla

The shell $\delta_{13}\text{C}$ values reveal a significant increase in C_4 vegetation whereas the shell $\delta_{18}\text{O}$ values reveal a notably dry period during the formation of unit 11 (about 130 ka). In contrast, snail data point to a higher proportion of C_3 plants and wetter conditions in sample 3 (marker red soil), in agreement with both pits from Lajares.

All in all, isotopic data from gastropod shells ($n = 104$) indicate that during the last two glacial cycles (between about 40 ka and 250 ka) moisture regimes and vegetation cover (in terms of C_3/C_4 type plant ratio) have fluctuated in northern Fuerteventura. The shell $\delta_{18}\text{O}$ values from our red marker soil (unit 9 in Fig. 9) from all four pits exhibit similar average results (ranging from +0.8‰ to +1.2‰). This suggests that the red marker soil was formed at comparable humidity levels in all pits, pointing to relatively homogenous moisture conditions across localities regardless of variations in topography. This finding further supports our stratigraphic correlations in the field. In contrast, the shell $\delta_{13}\text{C}$ values were more variable between pits. For example, in our red marker soil (unit 9, see Fig. 9), average $\delta_{13}\text{C}$ values ranged from –2.5‰ to –4.7‰, suggesting that variations in the vegetation cover show a marked spatial variability as observed today in present ecosystems of Fuerteventura.

5. Discussion and interpretation

This paper presents a standard stratigraphy based on a detailed multiproxy approach applied to four sand pits that are situated close to the village of Lajares (Northern Fuerteventura, Fig. 1).

The studied sand-paleosol-sequences are the result of a geomorphic cycle that was recurrent for several times during the Pleistocene. We assume a process cycle that starts with the formation of climbing dunes. These dunes were formed on the windward part of volcano cones. During heavy rains the uppermost parts of the dunes occasionally underwent erosion so that sand material could be deposited in toe slope position. Soil formation took place when sand supply was reduced. These soils could be eroded during erosive rainfall events, resulting in the deposition of soil sediment in toe slope position. Soil sediments and re-deposited sand from toe slope position, in addition to coastal shelf sand, delivered new sand for the next dune generation. Erosional unconformities within the sequences show the recurrence of erosional

phases during Pleistocene, which resulted in strongly reworked dune sand-paleosol sections.

Based on our chemical analyses conducted we can only distinguish between soil and soil sediment by slightly different CaCO_3 -contents that are slightly lower in soils. Discrimination is much easier during fieldwork, where soil sediments are characterized by their homogeneous color, the presence of lapilli and basaltic rock fragments and by a chaotic bedding of anthropod nests and molluscs. In contrast, soils that were formed in situ show a decrease in color intensity downwards, a mollusk arrangement in the upper part, and well-oriented anthropod nests in the lower part of the soil. These features are visible as well when soils developed in soil sediments.

Preliminary IRSL dating provides the chronologic framework and results point to a formation of the upper part of the sequences during the last ca. 250 ka. Between ca. 250 ka and ca. 50 ka about seven soils were formed (one in unit 9, two in unit 10, one in unit 11, two in unit 12 and one in unit 13), two of them showing features of strong soil formation (unit 9 and unit 12). This suggests that soil formation, dune sand accumulation and intensive erosion processes took place during glacial times, in agreement with Suchodoletz et al. (2010). However, age underestimates cannot be ruled out, as explained above. The Eemian interglacial short period (at ca. 125 ka) is not detectable by IRSL-dating in the Fuerteventura sequences as yet.

Snail isotopic data from soil horizons reflect slight changes in environmental conditions in the eastern Canary Islands associated with climate shifts (stadial-interstadial changes?; see Yanes et al., 2011, 2013b). However, our chronometric resolution is not yet precise enough to detect short oscillations in time. Thus, we do not know exactly when sand was delivered to the inner part of the island. Usually, sand mobility should have happened during stadial periods when the shelf was sufficiently exposed. However, if climate was humid during those phases, the shelf area should have been rapidly covered by vegetation, which may have reduced the time span of sand availability. In any case we distinguish three main phases of geomorphic processes regardless of their duration. These are sand supply, erosion and soil formation. Two geomorphic active processes such as sand supply with resulting dune formation and erosion probably took place under the same conditions. Both processes are favored by a reduced vegetation cover and could have happen within a relatively short time span. Unfortunately, the time resolution available is too coarse as a consequence of the poor properties of the dated material.

The third process is the formation of soils that is attributed to geomorphic stability. The intercalated soil horizons vary in color, thickness and isotopic composition of the shells preserved therein, all indicating slightly different intensities of pedogenesis and moisture regimes. It is proposed that differing soil formation intensity should be more related to exposure times than to climate conditions. The longer the duration of stable geomorphic conditions (with reduced sand supply), the stronger the soil formation features will be. This thesis should be included into the time model, based on our IRSL-dating. Soil formation intensity has been a matter of long debates. However, intensity is defined in physics as a function of energy, time and surface. For soil formation intensity the following formula may thus be helpful:

$$I = (E/S) * t$$

where I = intensity, E = energy or rather climate, S = surface or area and t = the duration of time. Thus, assuming a constant climate that acts on the same surface, only the time span of energy flow has to be increased in order to obtain a higher intensity level of soil formation.

This time span is shortened when sand supply covers the soil surface. In other words, if two different volumes of sand material are affected by the same energy flow during the same time span, the resulting pedogenetic intensity will be strong if the accumulated sediment layer is thin, but weak if the accumulated sediment layer is thick. This implies that under the same climatic conditions, soil formation intensity is

a question of either duration of surface exposition or sand supply (see also Zech et al., 2013). Continuous sand supply hinders soil formation and shortens exposure time regardless of the climate. This, in turn, implies that climate change is not necessarily required to pass from dune sand accumulation conditions to soil formation conditions, as was previously thought (e.g. Rohdenburg, 1970). Even if we agree with the overall concept of morphodynamic stability versus activity and their consequences as described by Rohdenburg (1970), it is not obvious that a change in morphodynamics must necessarily be due to climate change. According to this idea, soil formation intensity is primarily a function of the duration of a stable surface. In addition, the silt content in soils attributed to Saharan dust input may be an indication of the duration of soil formation, if the silt content is not related to weathering of the fine sand. This, however, could be deduced from kaolinite content in the soils because kaolinite content is a proxy for dust transport mainly from Sahel regions (Caquineau et al., 1998). All these features could help to estimate the duration of soil formation phases by means of intensity levels, thereby improving our time model.

Isotopic signals from snail shells show that every soil throughout the last glacial cycles (Figs. 5–8) was formed under slightly different climatic conditions. Shell assemblages were collected only from soils because snails were less abundant in sand horizons. Therefore, paleoenvironmental inferences (i.e. paleohumidity and paleovegetation) were solely deduced for soil formation phases when snails were abundant. Isotopic signals from snail shells suggest that not all paleosols were formed under equivalent climatic conditions. Indeed, our red marker soil (unit 9, Fig. 9) appears to have been developed under wetter conditions than the horizon immediately above (top of unit 10) and some older soils (e.g. unit 6). This may, in part, explain variations in the thickness and the geochemistry of the studied glacial soils here.

Dune sand accumulation and erosion are assumed to be short-term processes, attributed to increased sand supply (e.g. by a sudden drop of the sea level) and lower vegetation density on the dunes due to complicated growing conditions during sand delivery. However, heavy rains are likely during erosion phases as well. Eroded material (sand and soil sediments) will cover toe slopes and will also disturb vegetation. Thus, a self-amplifying process may even increase morphodynamic activity during such periods.

We subdivided the studied time span of the last ca. 250 ka into several short-term phases of morphodynamic activity and long-term phases of stability. The intensity degree of soil formation processes can be linked to the duration of the soil formation phase. From our previous studies on Lanzarote Island (Suchodoletz et al., 2009, 2010) and the eastern Canary Islands (Yanes et al., 2011, 2013b) we deduce wetter conditions during most of the last glacial cycle with respect to present climate.

Published alkenone proxy data from deep-sea cores close to the Canary Islands suggest that temperatures during much of the last glacial period were only ~ 4 °C lower than today (Zhao et al., 1995; Bard, 2002). This suggests that air temperatures during last glacial soil formation periods were probably around 16 °C, on average. Even if we overestimate that temperature drop during the last glacial cycle, soil-forming conditions in terms of mean annual temperature were still very favorable. The decisive climatic element that favors soil formation is, however, precipitation. In comparison to the contemporary climate that allows the formation of nebkha dunes and entisols, and based on our findings from Lanzarote and other eastern Canary Islands, a more humid climate during the last glacial cycles is the most plausible hypothesis (Yanes et al., 2011). The reason for geomorphic change, however, even if not long-lasting, still remains unclear.

6. Conclusions and future research plan

The present work integrates and revises the stratigraphy, geochronology, geochemistry and terrestrial gastropod isotope composition of four Pleistocene (from Holocene to ca. 250 ka) eolian sections in

northern Fuerteventura. For the first time, a stratigraphic standard profile for Northern Fuerteventura is presented and supported by IRSL ages. During the last ca. 250 ka, at least five important soil formation periods were identified. It is proposed that glacial soil-formation processes in Fuerteventura were primarily the result of (1) long-lasting exposure time, (2) geomorphic stability and (3) enhanced moisture conditions.

Isotopic data from terrestrial gastropod shells suggest that humidity fluctuated during the investigated time span, but often was higher than at present times. Likewise, published data from Lanzarote (Suchodoletz et al., 2009, 2010) also point to wetter conditions than today during much of the Pleistocene. Hence, even though air temperatures were cooler, snapshots of enhanced humidity and high exposure time permitted soil development during the middle and late Pleistocene on this subtropical island.

Future work aims to establish a finer time resolution by intensifying field-sampling collection and by sieving more sediment material to extract sufficient quartz grains and obtain an adequate amount of suitable material for OSL dating. In addition, new dating methods (post IR-IRSL; cf. Thiel et al., 2011) will be tested to reach deeper time levels and fading tests will be performed for the few samples with sufficient material available. Furthermore, clay mineralogical analysis will be conducted to better quantify the kaolinite content in the soils.

Further detailed measurements of environmental magnetism, such as anhysteretic remanent magnetisation and isothermal remanent magnetisation, will help to estimate the duration of soil forming periods. Future goals include additional fieldwork and sampling to assure and complete our first stratigraphic and paleoenvironmental results.

Acknowledgments

We are indebted to Dr. Constantino Criado for showing us these interesting profiles. We appreciate the intense discussions with M. and R. Zech about soil forming intensity and climate-driven weathering. We thank Siggí Gerstenhauer and Beate Winkler for laboratory work at the TU Dresden and Manfred Fischer for supporting luminescence dating at the University of Bayreuth. Financial support was provided by the German Research Foundation (Zo 51/33-1; FA 239/15-1) and the Spanish Ministry of Economía y Competitividad (Mineco) grant (CGL2011-29898/BTE). We would like to thank two anonymous reviewers for helpful comments.

References

- Barbouth, A., Rastin, B.C., 1983. A study of the absolute intensity of muons at sea level and under various thickness of absorber. *J. Phys. G: Nucl. Part. Phys.* 9, 1577–1595.
- Bard, E., 2002. Abrupt climate changes over millennial time scales: climate shock. *Phys. Today* 55, 32–38.
- Bouab, N., 2001. Application des méthodes de datation par luminescence optique à l'évolution des environnements désertiques – Sahara occidental (Maroc) et Iles Canaries orientales (Espagne) (Thèse). Université du Québec à Chicoutimi.
- Bouab, N., Lamothe, M., 1997. Geochronological Framework for the Quaternary Paleoclimatic Record of the Rosa Negra Section (Fuerteventura – Canary Islands, Spain). In: Meco, J., Petit-Maire, N. (Eds.), *Climates of the Past, Proceedings of the CLIP Meeting Held in June 2–7, 1995 – Lanzarote und Fuerteventura (Canary Islands, Spain)*. IUGS-UNESCO, Las Palmas de Gran Canaria, pp. 37–42.
- Bozzano, G., Kuhlmann, H., Alonso, B., 2002. Storminess control over African dust input to the Moroccan Atlantic margin (NW Africa) at the time of maxima boreal summer insolation: a record of the last 220 kyr. *Palaeogeogr. Palaeoclimatol. Palaeoecol.* 183, 155–168.
- Caquineau, S., Gaudichet, A., Gomes, L., Magonthier, M.C., Chatenet, B., 1998. Saharan dust: clay ratio as a relevant tracer to assess the origin of soil-derived aerosols. *Geophys. Res. Lett.* 25 (7), 983–986.
- Coello, J.J., Castillo, C., González, E.M., 1999. Stratigraphy, chronology, and palaeoenvironmental reconstruction of the quaternary sedimentary infilling of a volcanic tube in Fuerteventura, Canary Islands. *Quat. Res.* 52, 360–368.
- Criado, C., Dorta, P., 2003. An unusual, 'blood rain' over the Canary Islands (Spain). *The storm of January 1999*. *J. Arid Environ.* 55, 765–783.
- Criado, C., Torres, J.M., Hansen, A., Lillo, P., Naranjo, A., 2011. Intercalaciones de polvosahariano en paleodunas bioclasticas de Fuerteventura (Islas Canarias). *Cuat. Geomorfol.* 26 (1–2), 73–88.
- Damnati, B., Petit-Maire, N., Fontugne, M., Meco, J., Williamson, D., 1996. Quaternary palaeoclimates in the eastern Canary Islands. *Quat. Int.* 31, 37–46.

- Dearing, J., 1999. Environmental magnetic susceptibility. Using the Bartington MS2 System. Bartington Instruments. ISBN: 0952340909.
- Duchaufour, P., 1982. *Pedology. Pedogenesis and Classification*. Allen & Unwin, London, Boston, Sydney (448 pp.).
- Duller, G.A.T., 2007. Assessing the error on equivalent dose estimates derived from single aliquot regenerative dose measurements. *Ancient TL* 25, 15–24.
- Faust, D., Zöller, L., Suchodoletz, H.v., 2014. Comments on: palaeoclimatic considerations of talus flatirons and aeolian deposits in Northern Fuerteventura volcanic island (Canary Islands, Spain); authors: M. Gutiérrez-Elorza et al. 2011. *Geomorphology (Geomor-3811R3)*.
- Fitzsimmons, K.E., Magee, J.W., Amos, K.J., 2009. Characterisation of aeolian sediments from the Strzelecki and Tirari Deserts, Australia: implications for reconstructing palaeoenvironmental conditions. *Sediment. Geol.* 218, 61–73.
- Fuchs, M., Straub, J., Zöller, L., 2005. Residual luminescence signals of recent river flood sediments: a comparison between quartz and feldspar of fine- and coarse-grain sediments. *Ancient TL* 23, 25–30.
- Guerin, G., Mercier, N., Adamiec, G., 2011. Dose rate conversion factors update. *Ancient TL* 29, 5–8.
- Gutiérrez-Elorza, M., Lucha, P., Gracia, F.J., Desir, G., Marín, C., Petit-Maire, N., 2013. Palaeoclimatic considerations of talus flatirons and aeolian deposits in Northern Fuerteventura volcanic island (Canary Islands, Spain). *Geomorphology* 197, 1–9.
- Huot, S., Lamothe, M., 2003. Variability of infrared stimulated luminescence properties from fractured feldspar grains. *Radiat. Meas.* 37, 499–503.
- Koopmann, B., 1981. Sedimentation von Sahara-Staub im subtropischen Nordatlantik während der letzten 25 000 Jahre. *Meteor.-Forschung C/35*, 23–59.
- Lang, A., Wagner, G.A., 1997. Infrared stimulated luminescence dating of Holocene colluvial sediments using the 410 nm emission. *Quat. Sci. Rev.* 16, 393–396.
- Meco, J., Pomel, R., 1985. Les formations marines et continentales intervolcaniques des Iles Canaries orientales (Grande Canarie, Fuerteventura et Lanzarote): Stratigraphie et signification paléoclimatique. *Estud. Geol.* 41, 223–227.
- Meco, J., Petit-Maire, N., Fontugne, M., Shimmield, G., Ramos, A.J., 1997. The Quaternary deposits in Lanzarote and Fuerteventura (Eastern Canary Islands, Spain): an overview. In: Meco, J., Petit-Maire, N. (Eds.), *Climates of the Past, Proceedings of the CLIP Meeting Held in June 2–7, 1995 – Lanzarote und Fuerteventura (Canary Islands, Spain)*. IUGS-UNESCO, Las Palmas de Gran Canaria, pp. 123–136.
- Meco, J., Ballester-Santos, J., Perera-Betancort, M.A., Marrero-Romero, R., Niz-Guadalupe, G., Pallarés-Padilla, A., 2002. Paleoclimatología de Lanzarote y La Graciosa (yacimientos paleontológicos). *Servicio de Patrimonio Histórico del Cabildo de Lanzarote* (83 pp.).
- Meco, J., Betancort, J.F., Ballester, J., Fontugne, M., Guillou, H., Scaillet, S., Lomoschitz, A., Cilleros, A., Carracedo, J.C., Petit-Maire, N., Ramos, A., Perera-Betancort, M.A., Soler-Onís, E., Medina, P., Montesinos, M., 2008. *Historia Geológica del Clima en Canarias*. Las Palmas.
- Menéndez, I., Diaz-Hernandez, J.L., Manga, S.J., Alonso, I., Sanchez-Soto, P.J., 2007. Airborne dust accumulation and soil development in the North-East sector of Gran Canaria (Canary Islands, Spain). *J. Arid Environ.* 71, 57–81.
- Muhs, D.R., 2013. The geologic records of dust in the Quaternary. *Aeolian Res.* 9, 3–48. NASA: <http://earthobservatory.nasa.gov>; 1997.
- Ortiz, J.E., Torres, T., Yanes, Y., Castillo, C., De la Nuez, J., Ibáñez, M., Alonso, M.R., 2006. Climatic cycles inferred from the aminostratigraphy and amino-chronology of Quaternary dunes and paleosols from the eastern islands of the Canary Archipelago. *J. Quat. Sci.* 21, 287–306.
- Petit-Maire, N., Delibrias, G., Meco, J., Pomel, S., Rosso, J.C., 1986. Paléoclimatologie des Canaries orientales (Fuerteventura). *C. R. Acad. Sci.* 303 (13), 1241–1246 (Série II).
- Preusser, F., 2003. IRSL dating of K-rich feldspars using the SAR protocol: comparison with independent age control. *Ancient TL* 21, 17.
- Preusser, F., Degering, D., Fuchs, M., Hilgers, A., Kadereit, A., Klagen, N., Krbetschek, M., Richter, D., Spencer, J.Q.G., 2008. Luminescence dating: basics, methods and applications. *Eiszeitalter und Gegenwart J. Quat. Sci.* 57, 95–149.
- Rognon, P., Coudé-Gaussen, G., Le Coustumer, M.N., Balouet, J.C., Occhietti, S., 1989. Le massif dunaire de Jandía (Fuerteventura, Canaries): Évolution des paléoenvironnements de 20 000 BP à l'actuel. *Bull. Assoc. Fr. Etude Quat.* 1989 (1), 31–37.
- Rohdenburg, H., 1970. Morphodynamische Aktivitäts- und Stabilitätszeiten statt Pluvial- und Interpluvialzeiten-E&G. *J. Quat. Sci.* 21, 81–96.
- Roskin, J., Tsoar, H., Porat, N., Blumberg, D.G., 2011. Palaeoclimate interpretations of Late Pleistocene vegetated linear dune mobilization episodes: evidence from the northwestern Negev Dunefield, Israel. *Quat. Sci. Rev.* 30, 3364–3380.
- Roskin, J., Ktra, I., Porat, N., Zilberman, E., 2013. Evolution of Middle to Late Pleistocene sandy calcareous paleosols underlying the northwestern Negev Desert Dunefield (Israel). *Palaeogeogr. Palaeoclimatol. Palaeoecol.* 387, 134–152.
- Rothe, P., 1996. *Kanarische Inseln. Sammlung Geologischer Führer*. Gebrüder Bornträger, Berlin, Stuttgart (307 pp.).
- Rother, H., Shulmeister, J., Rieser, U., 2010. Stratigraphy, optical dating chronology (IRSL) and depositional model of pre-LGM glacial deposits in the Hope Valley, New Zealand. *Quat. Sci. Rev.* 29, 576–592.
- Schlichting, E., Blume, H.P., Stahr, K., 1995. *Bodenkundliches Praktikum*. Blackwell, Berlin, Wien (295 pp.).
- Singhvi, A.K., Krbetschek, M.R., 1996. Luminescence dating: a review and a perspective for arid zone sediments. *Ann. Arid Zone* 35, 249–279.
- Smalley, I., O'Hara-Dhand, K., McLaren, S., 2013. The nature and formation of aeolian mineral dust material. *Geophysical Research Abstracts* vol. 15. EGU.
- Stuut, J.B., Zabel, R., Ratmeyer, V., Helmke, P., Scherfuß, E., Lavik, G., Schneider, R., 2005. Provenance of present-day eolian dust collected off NW Africa. *J. Geophys. Res.* 110, D04202.
- Suchodoletz, H.v., Fuchs, M., Zöller, L., 2008. Dating Saharan dust deposits at Lanzarote (Canary Islands) by luminescence dating techniques and their implication for paleoclimate reconstruction of NW Africa. *Geochim. Geophys. Geosyst.* 9. <http://dx.doi.org/10.1029/2007GC001658>.
- Suchodoletz, H.v., Kühn, P., Hambach, U., Dietze, M., Zöller, L., Faust, D., 2009. Loess-like and palaeosol sediments from Lanzarote (Canary Islands/Spain) – indicators of palaeoenvironmental change during the Late Quaternary. *Palaeogeogr. Palaeoclimatol. Palaeoecol.* 278, 71–87.
- Suchodoletz, H.v., Oberhänsli, H., Hambach, U., Zöller, L., Fuchs, M., Faust, D., 2010. Obliquity controlled soil moisture fluctuations recorded in Saharan dust deposits on Lanzarote (Canary Islands) during the last 180 ka. *Quat. Sci. Rev.* 29 (17–18), 2173–2218.
- Suchodoletz, H.v., Blanchard, H., Hilgers, A., Radtke, U., Fuchs, M., Dietze, M., Zöller, L., 2012. TL and ESR dating of Middle Pleistocene lava flows on Lanzarote Island, Canary Islands (Spain). *Quat. Geochronol.* 9, 54–64.
- Suchodoletz, H.v., Zöller, L., Hilgers, A., Radtke, U., Faust, D., 2013. Vegas and dune palaeosol-sequences – two different palaeoenvironmental archives on the eastern Canary Islands. In: Fernandez-Palacios (Ed.), *Climate change Perspectives From the Atlantic. Past, Present and Future*. Servicio de Publicaciones, Universidad de la Laguna de Tenerife, pp. 259–274.
- Thiel, C., Buylaert, J.P., Murray, A.S., Terhorst, B., Hofer, I., Tsukamoto, S., Frechen, M., 2011. Luminescence dating of the Stratzing loess profile (Austria) – testing the potential of an elevated temperature post-IR IRSL protocol. *Quat. Int.* 234, 23–31.
- Torrent, J., Schwertmann, U., Schulze, D.G., 1980. Iron oxid mineralogy of some soils of two river terrace sequences in Spain. *Geoderma* 23, 191–208.
- Tripaldi, A., Forman, S.L., 2007. Geomorphology and chronology of Late Quaternary dune fields of western Argentina. *Palaeogeogr. Palaeoclimatol. Palaeoecol.* 251, 300–320.
- Yanes, Y., Delgado, A., Castillo, C., Alonso, M.R., Ibáñez, M., De la Nuez, J., Kowalewski, M., 2008. Stable isotope ($\delta_{18}O$, $\delta_{13}C$, and δD) signatures of recent terrestrial communities from a lowlatitude, oceanic setting: endemic land snails, plants, rain, and carbonate sediments from the eastern Canary Islands. *Chem. Geol.* 249, 277–292.
- Yanes, Y., Romanek, C.S., Delgado, A., Brant, H.A., Noakes, J.E., Alonso, M.R., Ibáñez, M., 2009. Oxygen and carbon stable isotopes of modern land snail shells as environmental indicators from a low-latitude oceanic island. *Geochim. Cosmochim. Acta* 73, 4077–4099.
- Yanes, Y., Yapp, C.J., Ibáñez, M., Alonso, M.R., De la Nuez, J., Quesada, M.L., Castillo, C., Delgado, A., 2011. Pleistocene–Holocene environmental change in the Canary Archipelago as inferred from stable isotopes of land snail shells. *Quat. Res.* 65, 658–669.
- Yanes, Y., Asta, M., Ibáñez, M., Alonso, M.R., Romanek, C.S., 2013a. Palaeoenvironmental implications of carbon stable isotope composition of land snail tissues. *Quat. Res.* 80, 596–605.
- Yanes, Y., Garcia-Alix, A., Asta, M.P., Ibáñez, M., Alonso, M.R., Delgado, A., 2013b. Late Pleistocene–Holocene environmental conditions in Lanzarote (Canary Islands) inferred from calcitic and aragonitic land snail shells and bird bones. *Palaeogeogr. Palaeoclimatol. Palaeoecol.* 378, 91–102.
- Zech, R., Zech, M., Markovic, S., Hambach, U., Yongsong, H., 2013. Humid glacials, arid interglacials? Critical thoughts on pedogenesis and paleoclimate based on multi-proxy analyses of the loess-paleosol sequence Crevenka, Northern Serbia. *Palaeogeogr. Palaeoclimatol. Palaeoecol.* 387, 165–175.
- Zhao, M., Beveridge, N.A.S., Shackleton, N.J., Sarnthein, M., Eglinton, G., 1995. Molecular stratigraphy of cores off northwest Africa: sea surface temperature history over the last 80 ka. *Paleoceanography* 10, 661–675.
- Zielhofer, C., Recio Espejo, J.M., Núñez Granados, M., Faust, D., 2009. Durations of soil formation and soil development indices in a Holocene Mediterranean floodplain. *Quat. Int.* 209 (1–2), 44–65.
- Zöller, L., 1995. *Würm- und Riß/Loess-Stratigraphie und Thermolumineszenz-Datierung in Süddeutschland und angrenzenden Gebieten*. Habilitation. Fakultät für Geowissenschaften. Heidelberg, Ruprecht-Karls-Universität Heidelberg (224 pages).